Room-temperature, wide-band, quantum well infrared photodetector for microwave optical links at 4.9 μm wavelength

Rodriguez, Etienne; Mottaghizadeh, Alireza; Gacemi, Djamal; Palaferri, Daniele; Asghari, Zahra; Jeannin, Mathieu; Vasanelli, Angela; Bigioli, Azzurra; Todorov, Yanko; Beck, Mattias; Faist, Jerome; Wang, Qi Jie; Sirtori, Carlo

2018

Rodriguez, E., Mottaghizadeh, A., Gacemi, D., Palaferri, D., Asghari, Z., Jeannin, M., ... Sirtori, C. (2018). Room-temperature, wide-band, quantum well infrared photodetector for microwave optical links at 4.9 μm wavelength. ACS Photonics, 5(9), 3689-3694. doi:10.1021/acsphotonics.8b00704

https://hdl.handle.net/10356/137485

https://doi.org/10.1021/acsphotonics.8b00704

Room temperature, wide-band Quantum Well Infrared Photodetector for microwave optical links at 4.9 µm wavelength

Etienne Rodriguez,[1,2*] Alireza Mottaghizadeh,[3] Djamal Gacemi,[3] Daniele Palaferri,[3] Zahra Asghari,[3] Mathieu Jeannin,[3] Angela Vasanelli,[3] Azzurra Bigioli,[3] Yanko Todorov,[3] Mattias Beck,[4] Jerome Faist,[4] Qi Jie Wang,[1,2*] and Carlo Sirtori[1,3*]

[1]School of Electrical and Electronic Engineering, Nanyang Technological University, 639798, SINGAPORE

[2]CINTRA CNRS/NTU/THALES, UMI 3288, Research Techno Plaza, 50 Nanyang Drive, Border Block, Level 6, 637553, SINGAPORE

[3]Université Paris Diderot, Sorbonne Paris Cité, Laboratoire Matériaux et Phénomènes Quantiques, UMR7162, 75013 Paris, France

[4]ETH Zurich, Institute of Quantum Electronics, Auguste-Piccard-Hof 1, Zurich 8093, Switzerland

**Email:* etienne.rodriguez@gmail.com, qjwang@ntu.edu.sg and carlo.sirtori@univ-paris-diderot.fr

High-speed room temperature quantum well infrared photodetectors (QWIPs) at λ ~ 4.9 µm have been realised in a strain compensated $In_{0.1}Ga_{0.9}As/Al_{0.4}Ga_{0.6}As$ heterostructure grown on a GaAs substrate. The high-speed properties at room temperature have been optimised by using a specifically designed air-bridge structure which greatly reduces the time constant of the effective RC circuit, thus allowing transmission and detection of high-frequency signals. By modulating a high-speed quantum cascade laser (QCL) centred at λ ~ 4.7 µm we were able to record a modulation of the photocurrent up to ~26 GHz, which is limited by our setup. At 300 K and under a bias voltage of –5 V our device shows high responsivity and detectivity of 100 mA/W and 1 x 10^7 Jones, respectively. The developed high-performance QWIPs at this wavelength are highly promising for optical heterodyne measurement, high-speed free space communications in microwave optical links and frequency comb QCLs characterisations.

Keywords: Quantum devices, Mid-infrared, Photodetectors, Ultrafast devices.

Recent developments in high-speed mid-infrared (mid-IR) photonics such as free-space optical communications and frequency combs laser characterization, have placed a high demand on high performance high-speed mid-IR photodetectors. Technologies based on HgCdTe and InSb have made good progress in achieving high-responsivity and high-sensitivity photodetectors [1,2].

However, they often operate at low operating temperatures and possess a relatively low-frequency bandwidth which makes them not suitable for high-speed applications.[3] Photodetectors based on intersubband transitions, i.e. quantum well infrared photodetector (QWIP) and quantum cascade detectors (QCDs), have also shown remarkable performance in both mid-wavelength infrared (MWIR) (~3-7 µm) and long-wave infrared (LWIR) (~7-14 µm). Due to their high photoconductive gain and high-speed operation, QWIPs have attracted significant attention.[4] This photodetector technology has the advantages of high absorption,[5] wide tunability of the detection wavelength based on band-structure engineering of the quantum structures,[6] and high-speed behaviour due to their intrinsic short carrier lifetime.[7,8] This physical parameter is an inherent characteristic of the intersubband transitions which leads to high-frequency response exceeding 100 GHz[8] and a very high saturation intensity[9] allowing a wide range of applications including heterodyne detection,[8,10,11] characterisation of ultrafast laser pulses[12] and wideband free space communications.[13]

The development of QWIP has been successful in both the MWIR and LWIR bands.[2,14] Great efforts have been devoted to the development of LWIR QWIPs. It was used to detect the beating signals between two CO_2 lasers at a frequency starting from 35 GHz up to 110 GHz at 10 µm.[8] Recently, ultrahigh-sensitivity heterodyne measurements in QWIP at room temperature have been demonstrated using metamaterials to enhance light-matter interactions and significantly increase signal-to-noise ratio.[11] On the other hand, in the MWIR region, high responsivity of 1 A/W[15] and background-limited detectivity of 2×10^{11} Jones[16] have been demonstrated but only at cryogenic temperatures. As far as we know no prior work has been devoted to high-speed and high performance QWIPs in the MWIR region at room temperature.

In this work, we have demonstrated a direct modulation of high-speed QWIP up to 26 GHz at room temperature. The active region of the QWIP is made of 40 periods of strain-compensated $In_{0.1}Ga_{0.9}As/Al_{0.4}Ga_{0.6}As$ alloy grown on GaAs substrate and operate at 4.9 µm. We designed a 25 µm square MESA where the top contact is realised with an air-bridge structure for high-frequency modulations. A high-speed QCL[17] that can be modulated up to 26 GHz was used to measure the frequency response of our QWIP device and to detect the beatnote signals at 11.5 and 23.1 GHz. Moreover, we also used rectification techniques to measure the frequency response of the QWIP up to 30 GHz, where the signal is attenuated by approximately 10 dBm. The rectified response is consistent with the direct-modulated QCL measurement.

STRUCTURE, SAMPLE DESCRIPTION AND TEMPERATURE CHARACTERISTICS

The QWIP wafer was grown by molecular beam epitaxy on a GaAs substrate. The active layers are composed of 40 periods of the following sequence: 5 Å $In_{0.1}Ga_{0.9}As$, 25 Å $In_{0.1}Ga_{0.9}As$ (doped: 5×10^{11} cm^{-2}), and 5 Å $In_{0.1}Ga_{0.9}As$ separated by a 400 Å $Al_{0.4}Ga_{0.6}As$ barrier. The active region is sandwiched between two highly-doped GaAs contact layers as it is drawn in Fig. 1.

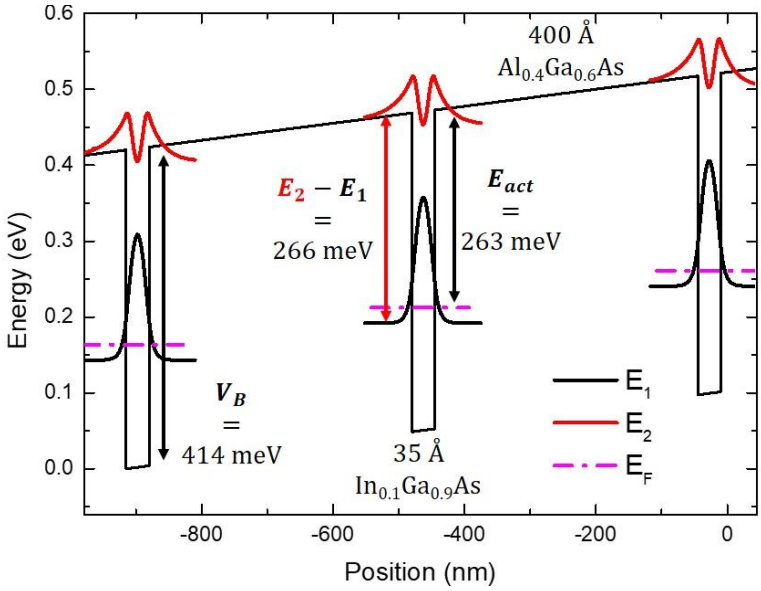

Fig. 1. *Band-structure of the developed qauntum well infrared photodetector (QWIP) with 3 quantum wells (QWs) active regions at a bias voltage of 2 V. The most relavant physical parameters of the sructure are indicated in the figure.*

The bandstructure and relevant energy levels of the detector are displayed in Fig. 1 with E_1 the lower energy state, E_2 the upper energy state and E_F, E_{act} and V_B are respectively the Fermi level, the activation energy of the QW and the total barrier height. The upper energy level is in resonance with the top of the barrier, as in the typical bound-to-quasicontinuum design.

The fabrication of the devices has been conceived to achieve high-speed performances. Square mesas were defined using Inductively Coupled Plasma (ICP) etching system on an annealed Ge/Au/Ni/Au top contact up to the bottom contact. Then, we protected the mesas using a thick photoresist before removing the bottom contact where the coplanar waveguide will take place by wet-etching. The air-bridge metal structure is realised by using two different photoresists, one positive photoresist used as a pillow to support the ridge in front of the mesa, and the negative photoresist for the lift-off process, after the Ti/Au deposition by e-beam evaporation technique. The additional bakes of the positives photoresist are essential to soften the angles and to support the development of the negative photoresist. Moreover, the e-beam deposition must be done with three different angles (+30, 0 and -30 °) following the direction of the coplanar waveguide to ensure good adhesion between the bridge and the substrate. The air-bridge between the top of the mesa and the microstrip ensures a low time constant of the effective RLC circuit. The microstrip is widened to a width fitted to the high-frequency launcher. The top view of the device is shown Fig. 2 (a), where the inset shows clearly the squared mesa and the gold air-bridge. Finally, we polished the facet of the device at 45° to efficiently couple the light into the active region.

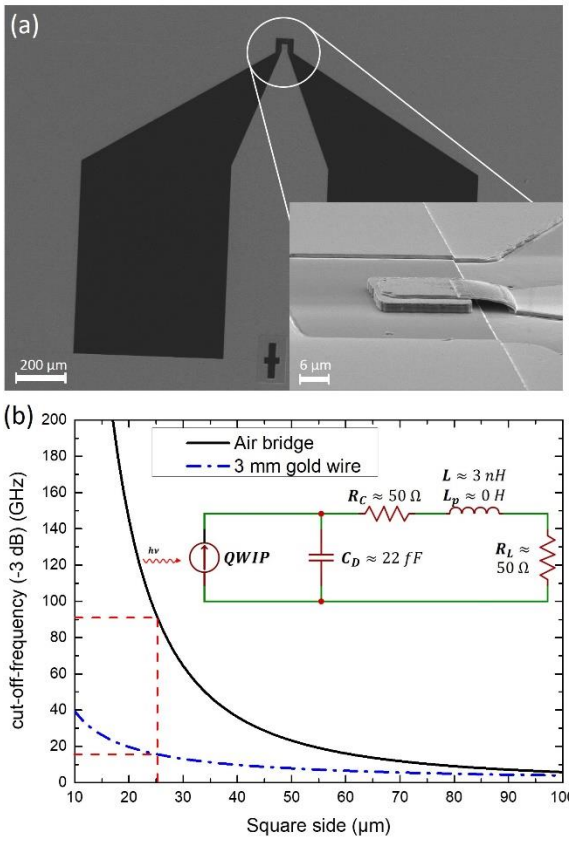

Fig. 2. *(a) The top view of the QWIP (The inset: zoom-in of the active region with the air bridge); (b) Cut-off frequency at –3 dB as a function of the MESA dimensions for the conventional wire bonding (dashed line) and the proposed air-bridge (solid line) devices (The inset: electrical circuit of the device).*

In order to optimise the electrical circuit for high speed operation, the wire inductance is suppressed by realising a contact with a small air-bridge connected to a 50 Ω microstrip line. The capacitance of the device is directly linked to the size of the mesa. Considering practical implementations, we designed a relatively small square mesa of 25 x 25 μm^2. This dimension corresponds to an electrical cut-off frequency of 92 GHz calculated using the equivalent electrical circuit model. Fig. 2 (b) illustrates the electrical cut-off frequency at –3 dB for 40 periods with wire bonding (dashed line) and with air-bridge (solid line) waveguides. The inset of Fig. 2 (b) shows the equivalent circuit where the QWIP is considered as a current generator. C_D represents the device capacitance, R_C is the access resistance of the coplanar line which is designed to be 50 Ohm to match the impedance of the system load R_L, and L is the inductance of the wire bonding (in the case of air-bridge the parasite inductance L_p is negligible).

The fabricated QWIP device is mounted on a cryostat and then cooled down at cryogenic temperatures. Photocurrents at different temperatures and bias voltages are measured by 1:1 imaging of the 0.2 inch aperture blackbody at 1000° C. In order to remove the dark current, the photon flux is chopped at 500 Hz, and the measurements are performed using a lock-in amplifier (Stanford Research SR830). The photocurrent amplitude is measured through a shunt resistance in series with the QWIP without the use of any pre-amplifier. We extracted the power on the

QWIP by using a calibrated MCT detector in the exact same configuration. Taking into account the dimensions and the spectral responses of the different photodetectors, the impinging power is 160 nW on the 25 µm square QWIP. The spectra are measured using a Bruker Fourier-transform infrared (FTIR) spectrometer with step scan technique. The signal from the detector is pre-amplified by a low-noise current amplifier (DLPCA-200) and sent to the lock-in amplifier.

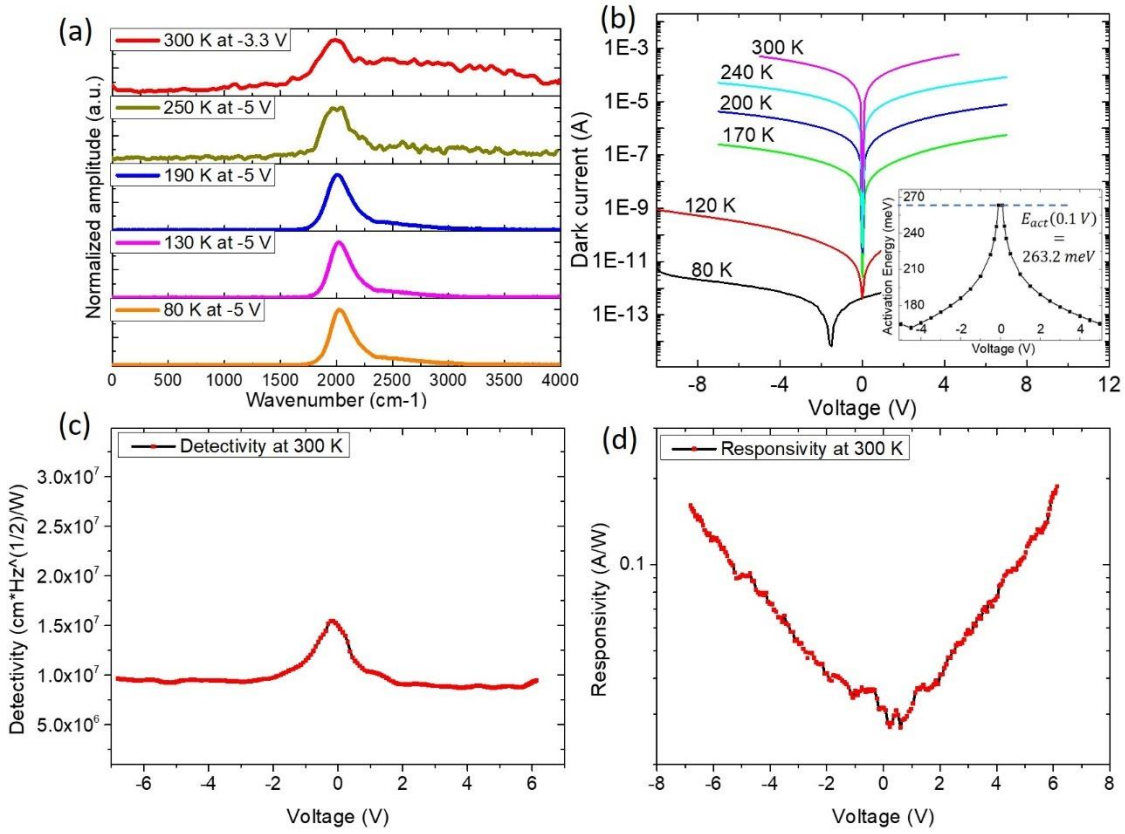

Fig. 3. *(a) Spectra of the QWIP at several different temperatures up to 300 K; (b) Current-voltage (IV) characteristics in background condition for different temperature, inset: activation energy as a function of the bias voltage; background-limited detectivity (c) and responsivity (d) of the QWIP device at 300 K as a function of the bias voltage.*

The internal IR source of the FTIR emit about 52 nW only, despite the low input optical power we were able to measure the response spectra at up to 300 K as shown in Fig. 3. (a). The spectra present an asymmetry, which corresponds to the intrinsic characteristic of the bound-to-quasicontinuum design.[18] With the increase of the temperature, the central wavelength of the QWIP slightly shifts towards the lower energy (from 2050 cm^{-1} at 80 K to 2010 cm^{-1} at 250 K due to the depolarization effect. The linewidth starts to increase from 130 K (from 27.03 meV up to 130 K to 33.48 meV at 250 K) due to the electron-phonon interactions. Fig. 3. (b) shows the evolution of the background current as a function of the voltage up to room temperature. The exponential fits of the evolution of the dark current with the temperature allowed the

calculation of the activation energy of the system which corresponds to 263.2 meV at low bias voltages. This energy is the thermal energy required to excite electrons from the Fermi energy to the continuum and is in a very good agreement with the activation energy simulated in Fig. 1.

The background-limited detectivity and the responsivity at 300 K as a function of the bias voltage are, respectively, shown in Figs. 3 (c) and (d). They exhibit a value of 100 mA/W and 1 x 10^7 Jones for a bias voltage of −5 V.

HIGH-SPEED BEHAVIOUR

The first high-speed characterizations of our QWIPs have been done by direct modulation of a QCL. The measurement setup is shown in Fig. 4 (a). A high-speed current modulated QCL at a wavelength of 4.7 µm is mounted in a high-speed cryostat and operates at cryogenic temperatures. A bias-T is used which allows the injection of the DC and the microwave currents simultaneously. The radiation from the laser is collected and then focused on the QWIP using two convex lenses. The output power of the laser corresponds to 110 mW, however, due to the small size of the detector, only a small fraction of the power is coupled with the QWIP. It results with a photocurrent of about 600 µA at room temperature. The QWIP is also connected through a bias-T in order to measure the modulated photocurrent of the QWIP at high-frequency using a spectrum analyser (Agilent E4407B) limited to 26.5 GHz. The injection is tuned from 100 MHz to 26.5 GHz using a signal generator (Anritsu MG3693B) with a step of 300 MHz at a RF power of –10 dBm.

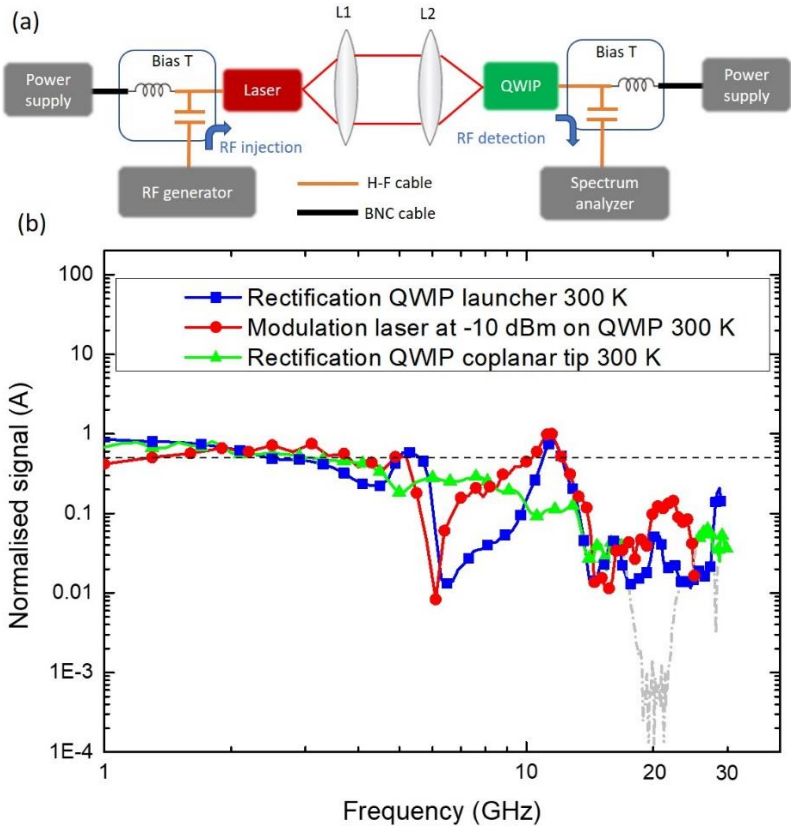

Fig. 4. *(a) The schematic illustration of the setup used to investigate the high-speed modulation of the QWIP. A high-speed direct-modulated quantum cascade laser (QCL) is used in the experiment; (b) Photoresponse of the QWIP with the QCL modulated at –10 dBm at 300 K (red line + symbol) at a bias voltage of –4 V. The rectification measurements of QWIP using the cryostat setup (blue line + symbol) and using the coplanar tip configuration (green line + symbol) with in dashed grey line the resonances due to parasitic effects of its electrical circuit. The black dashed line represents the value at -3 dB.*

To avoid microwave pick-ups, we separated the emitter and detector by more than a meter, and the power of the injected microwaves remains as low as possible. Furthermore, to remove the remaining antenna effects, we have detected the background by carrying out the same measurements but with laser beam blocked. All these measurements were realised at room temperature with a bias voltage on the QWIP at –4 V, while the laser operate at low temperature with a radio frequency (RF) injection power of –10 dBm as shown in Fig. 4 (b).

This approach is complementary with the detection of the beating signal shown in Fig. 5. In the direct modulation approach, the RF signal injected in the laser will modulate the IV curve of the laser according to the injected power. It is translated by an amplitude modulation of the laser intensity, which is then transmitted to the photodetector. Therefore, the amplitude modulation detected by the QWIP will also be dependent on the quality of the injection of the laser.

We also verified the high speed measurements by microwave rectification techniques utilising an RF launcher for the QWIP characterizations in the cryostat at 300 K. Due to the inherent non-linear I-V characteristics of QWIPs, microwave rectification technique is a way to study the roll-off behaviour of the QWIP by applying an RF signal to the photodetector and measuring the variation of its DC biasing current. This value reflects the frequency roll-off response of the device limited by the intrinsic-transport and the electrical parameters of the circuit.[5] Using this method, high speed characterizations of photodetectors are no longer limited by the spectrum analyser, but only by the synthesiser RF generator. With this, we can extend the high-speed measurement up to 30 GHz. This measurement has also been carried out by operating a lock-in amplifier technique with an electrical modulation of the RF signal using a signal generator. As a result, the RF injection is over modulated by a 10 kHz rectangular square wave with a duty cycle of 50% and sent to the QWIP though the bias-T with the bias voltage of the QWIP applied. The variation of the bias voltage is directly recovered at the terminal of the generator using a BNC-T and sent to the AC input of the lock-in amplifier synchronised with the signal generator.

The rectification measurements, displayed in Fig. 4 (b), exhibit good agreement with the direct modulation using the QCL modulated at –10 dBm, and show a frequency response up to 30 GHz. At 22 GHz the signal of the direct modulation is attenuated by approximately 8 dBm while at 30 GHz the rectification signal shows a diminution by approximately 10 dBm. We do not identify a clear change of the slope in the bode diagram of the rectification measurements or direct modulations which would correspond to the cut-off frequency. The resonances of our

system around 10 GHz are due to some parasitic effects in the electrical circuit using the launcher in the cryostat. We conducted the same measurements using a simpler electrical circuit composed of an RF coplanar tip, where these resonances were not shown as seen in green in Fig. 4 (b). However, this setup suffers from another resonance at higher frequencies represented in grey dashed line, also visible in the transmission line of the electrical circuit not displayed here.

APPLICATION ON FERQUENCY COMB QCL AND OPTICAL LINKS

The optical frequency combs have the potential to revolutionise the communication and especially the free-space communication in the atmospheric windows in the mid-IR where, recently, Joerg Pfeifle et al. has achieved a data transfer rate of 1.44 Tbit s^{-1} over up to 300 km by using frequency combs sources.[19] Our wide-band photodetector is designed to work up to RT in the MWIR. Therefore, it can be used in high-speed MWIR communication data and the characterisation of frequency comb laser by analysing the beatnote signal. The detection of the beating signal of the multimode laser is done by mixing the multiple modes in a high-speed mixer, i.e. QWIP. The frequency of this signal is directly related to the length of the cavity but also to the dispersion which makes it a powerful tool to study frequency combs lasers.

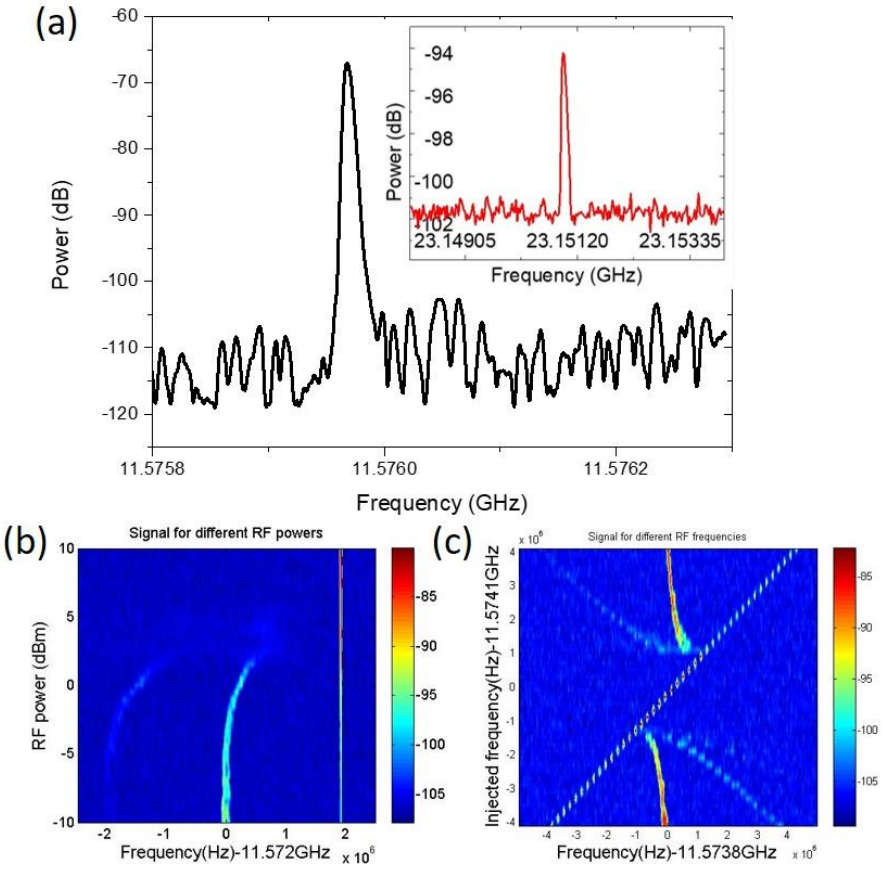

Fig. 5. *(a) The first harmonic of the beatnote, corresponding to the 3 mm laser, is collected on the QWIP at 300 K. The inset: the second harmonic of the beatnote at 23.15 GHz;*

injection-locking observed on the QWIP at 300 K by (b) increasing the injected power and (c) tuning the injection frequency on a 3 mm laser.

Moreover, as one of the important applications of mid-IR photonics, photodetectors could be used to characterise frequency comb lasers. We also detected the beatnote arising from the frequency mixing of longitudinal modes of our multimode laser. Fig. 5 (a) and the inset show the detection on the QWIP at 300 K of the first and second harmonic of the beatnote of a 3 mm laser corresponding respectively to a frequency of 11.58 and 23.15 GHz (the width at -3 dBm of the first harmonic of the beatnote is about 4 kHz). We also performed the injection-locking by increasing the injected power and the injected frequency on the laser as respectively displayed in Fig. 5 (b) and (c). We realised these measurements using a coplanar tip at room temperature. The RF signal injected near the round-trip frequency of the laser will act as a master oscillator and pull or inject the beating signal and therefore, impose the intermode frequency. The injection-locking is a power tool to achieve active mode-locking which stabilise the comb emission of the laser and can significantly broaden the emission spectrum by the generation and proliferation of sidebands in the optical range.[20,21] This method exhibits another direct method of high-frequency detection, same measurements were realised using the launcher configuration at low, and room temperature not shown here.

CONCLUSION

In conclusion, we have demonstrated that high speed QWIP at 4.9 µm with a modulation that goes up to 30 GHz at room temperature. Our high-speed QWIPs have a specific design for very high frequency based on small surface detector and air-bridges which enables the propagation and injection of high-frequency RF signals. It has been tested, up to room temperature, by direct and indirect method up to, respectively, 26 and 30 GHz both limited by the electrical systems. We also observed on the QWIP at room temperature the two first harmonics of the beating signal and the injection-locking of 3 mm lasers, which correspond to the beating signals at the frequency of 11.57 and 23.15 GHz, respectively. Beyond the high-speed behaviour of our devices, the intrinsic properties of intersubband transitions and their high responsivity at room temperature make them very promising for many applications in the 3 – 5 µm atmospheric window in the MWIR, especially in heterodyne detection, free-space communication and frequency comb QCLs characterisations.

Funding. Singapore National Research Foundation, Competitive Research Program (NRF-CRP18-2017-02) and Singapore Ministry of Education Tier 2 Program (MOE2016-T2-2-159).

Acknowledgement. We would like to thank Maria Amanti her useful discussions and suggestions on this work.

REFERENCES

(1) Norton, P. HgCdTe Infrared Detectors. *Opto-Electronics Rev.* **2002**, *10* (3), 159–174.

(2) Rogalski, A. Infrared Detectors: Status and Trends. *Prog. Quantum Electron.* **2003**, *27* (2–3), 59–210.

(3) Varesi, J. B.; Bornfreund, R. E.; Childs, A. C.; Radford, W. A.; Maranowski, K. D.; Peterson, J. M.; Johnson, S. M.; Giegerich, L. M.; De Lyon, T. J.; Jensen, J. E. Fabrication of High-Performance Large-Format MWIR Focal Plane Arrays from MBE-Grown HgCdTe on 4" Silicon Substrates. *J. Electron. Mater.* **2001**, *30* (6), 566–573.

(4) Liu, H. C. Photoconductive Gain Mechanism of Quantum-Well Intersubband Infrared Detectors. *Appl. Phys. Lett.* **1992**, *60* (12), 1507–1509.

(5) H. Schneider and H. C. Liu. Quantum Well Infrared Photodetectors. In *Springer Series in Optical Sciences*; 2007.

(6) Capasso, F. Band-Gap Engineering: From Physics and Materials to New Semiconductor Devices. *Science (80-.).* **1987**, *235* (4785), 172–176.

(7) Liu, H. C.; Li, J.; Buchanan, M.; Wasilewski, Z. R. High-Frequency Quantum-Well Infrared Photodetectors Measured by Microwave-Rectification Technique. *IEEE J. Quantum Electron.* **1996**, *32* (6), 1024–1028.

(8) Grant, P. D.; Dudek, R.; Buchanan, M.; Liu, H. C. Room-Temperature Heterodyne Detection up to 110 GHz with a Quantum-Well Infrared Photodetector. *IEEE Photonics Technol. Lett.* **2006**, *18* (21), 2218–2220.

(9) Vodopyanov, K. L.; Chazapis, V.; Phillips, C. C.; Sung, B.; Harris, J. S. Intersubband Absorption Saturation Study of Narrow III - V Multiple Quantum Wells in the Spectral Range. *Semicond. Sci. Technol.* **1997**, *12* (6), 708–714.

(10) Hofstetter, D.; Graf, M.; Aellen, T.; Faist, J.; Hvozdara, L.; Blaser, S. 23 GHz Operation of a Room Temperature Photovoltaic Quantum Cascade Detector at 5.35 Mm. *Appl. Phys. Lett.* **2006**, *89* (6), 2004–2007.

(11) Palaferri, D.; Todorov, Y.; Bigioli, A.; Mottaghizadeh, A.; Gacemi, D.; Calabrese, A.; Vasanelli, A.; Li, L.; Davies, A. G.; Linfield, E. H.; et al. Room-Temperature Nine-Mm-Wavelength Photodetectors and GHz-Frequency Heterodyne Receivers. *Nat. Publ. Gr.* **2018**, *556* (7699), 85–88.

(12) Hugi, A.; Villares, G.; Blaser, S.; Liu, H. C.; Faist, J. Mid-Infrared Frequency Comb Based on a Quantum Cascade Laser. *Nature* **2012**, *492* (7428), 229–233.

(13) R. Martini, R. Paiella, C. Gmachl, F. Capasso, E.A. Whittaker, H.C. Liu, H.Y. Hwang, D.L. Sivco, J. N. B. and A. Y. C. High-Speed Digital Data Transmission Using Mid-Infrared Quantum Cascade Lasers. *Electron. Lett.* **2001**, *37* (21).

(14) Schneider, H.; Maier, T.; Fleissner, J.; Walther, M.; Koidl, P.; Weimann, G.; Cabanski, W.; Finck, M.; Menger, P.; Rode, W.; et al. Dual-Band QWIP Focal Plane Array for the Second and Third Atmospheric Windows. *Infrared Phys. Technol.* **2005**, *47* (1–2), 53–58.

(15) Costard, E.; Bois, P.; Marcadet, X.; Nedelcu, A. QWIP Products and Building Blocks for High Performance Systems. *Infrared Phys. Technol.* **2005**, *47* (1–2), 59–66.

(16) Guériaux, V.; Nedelcu, A.; Bois, P. Double Barrier Strained Quantum Well Infrared Photodetectors for the 3–5 Mm Atmospheric Window. *J. Appl. Phys.* **2009**, *105* (11), 114515.

(17) Calvar, A.; Amanti, M. I.; Renaudat St-Jean, M.; Barbieri, S.; Bismuto, A.; Gini, E.; Beck, M.; Faist, J.; Sirtori, C. High Frequency Modulation of Mid-Infrared Quantum Cascade Lasers Embedded into Microstrip Line. *Appl. Phys. Lett.* **2013**, *102* (18), 1–4.

(18) Palaferri, D. Antenna Resonators for Quantum Infrared Detectors and Fast Heterodyne Receivers, University Paris Diderot - Paris 7, Laboratoire Matériaux et Phénomènes Quantique (MPQ), 2018.

(19) Pfeifle, J.; Brasch, V.; Lauermann, M.; Yu, Y.; Wegner, D.; Herr, T.; Hartinger, K.; Schindler, P.; Li, J.; Hillerkuss, D.; et al. Coherent Terabit Communications with Microresonator Kerr Frequency Combs. *Nat. Photonics* **2014**, *8* (5), 375–380.

(20) St-Jean, M. R.; Amanti, M. I.; Bernard, A.; Calvar, A.; Bismuto, A.; Gini, E.; Beck, M.; Faist, J.; Liu, H. C.; Sirtori, C. Injection Locking of Mid-Infrared Quantum Cascade Laser at 14 GHz, by Direct Microwave Modulation. *Laser Photonics Rev.* **2014**, *8* (3), 443–449.

(21) Li, H.; Laffaille, P.; Gacemi, D.; Apfel, M.; Sirtori, C.; Leonardon, J.; Santarelli, G.; Rösch, M.; Scalari, G.; Beck, M.; et al. Dynamics of Ultra-Broadband Terahertz Quantum Cascade Lasers for Comb Operation. *Opt. Express* **2015**, *23* (26), 33270.